Exosomal miRNA-328-3p Targets ZO-3 and Inhibits Porcine Epidemic Diarrhea Virus Proliferation

Zhao Han
Jilin Agricultural University
Yang Jinxin
Jilin Agricultural University
Wang Qian
Changchun University of Chinese Medicine
Cui Zhanding
Jilin Agricultural University
Li Dengliang
Jilin Agricultural University https://orcid.org/0000-0002-1085-5294
Niu Jiangting
Jilin Agricultural University
Guo Yanbing
Jilin Agricultural University
Zhang Qian
Jilin Agricultural University
Zhang Shuang
Jilin Agricultural University
Zhao Yanli
Jilin Agricultural University
Wang Kai
Jilin Agricultural University
Lian Wei
Jilin Zhengye Biological Products Co.,Ltd
Hu Guixue (huguixue901103@163.com)
Jilin Agricultural University

Research Article

Keywords: exosomes, microRNA328-3p, PEDV, tight junction protein ZO-3

Posted Date: February 23rd, 2021

DOI: https://doi.org/10.21203/rs.3.rs-231513/v1

Abstract

As essential transfer carriers for cell-to-cell communication and genetic material, exosomes carry microRNAs that participate in the regulation of various biological processes. MicroRNA is a type of single-stranded noncoding RNA that can bind to specific target gene mRNA to degrade or inhibit its translation, thereby regulating the expression of related target genes. At present, it is known that a variety of microRNAs are involved in the viral infection process, but there are few reports on research into the specific microRNAs involved in PEDV infection. In this study, we isolated and identified exosomes in PEDV-infected Vero E6 cells. Using transcriptomics technology, we found that miRNA-328-3p was significantly downregulated in exosomes following PEDV infection. Moreover, exosomal miRNA-328-3p inhibits cell infection by PEDV through targeting and inhibition of tight junction protein-3 (TJP-3/ZO-3) in recipient cells. Our findings provide evidence that after infecting cells, PEDV downregulates the expression of miRNA-328-3p, and the resulting reduced inhibition of the target ZO-3 protein helps to enhance PEDV infection. These results provide new insights for understanding the regulatory mechanism of PEDV infection.

Introduction

Porcine epidemic diarrhea virus (PEDV) belongs to the genus *Alphacoronavirus*, family *Coronaviridae*. It is an enveloped, single-stranded, positive-sense RNA virus. Porcine epidemic diarrhea (PED) is an acute and highly contagious enteric disease caused by PEDV, characterized by watery diarrhea, vomiting, and high mortality in suckling and nursing pigs. Some studies have shown that the S1 protein of PEDV is one of the most critical functional proteins that contributes to cell apoptosis [1]. PEDV structure protein envelope (E), membrane (M), nucleocapsid (N) protein, open reading frame 3 (ORF3),nonstructural proteins 1 (NSP1), NSP3, NSP7, NSP14, NSP15, and NSP16 were found to suppress interferon (IFN) activities to promote replication [2–5]. However, Luo et al. demonstrated that occludin plays an essential role in PEDV infection. Moreover, PEDV entry and occludin internalization seem to be closely coupled [6]. Occludin is a critical tight junction (TJ) protein. TJ is essential for the maintenance and repair of the intestinal mucosal barrier. The zonula occludens (ZO) family (including ZO-1–3) and the occludin and claudins family (including claudin-1–24 in pig) are essential TJ proteins. Zong et al. found that Occludin and Claudin-4 play an essential role in PEDV infection in piglets [7]. Jung et al. suggested that structurally impaired TJ and adherens junction (AJ) proteins were involved in the pathogenesis of PEDV [8]; PEDV + TGEV co-infection contributed more markedly to the damage of tight corners and remodeling of microfilaments than infection by either PEDV or TGEV alone [9]. In essence, the villous epithelium of the small intestine can maintain the integrity of the intestinal wall through tight junction proteins. PEDV infection has been found to destroy intestinal villi epithelial cells, reduce intestinal absorption capacity, and cause malabsorptive diarrhea.

Exosomes are small vesicles derived from different types of cells and are actively released into the extracellular space. Exosomes can transport proteins, mRNA, miRNA, and nucleic acids between cells and serve as mediators of intercellular communication [10]. Accumulating evidence suggests that exosomes derived from cells infected by certain viruses selectively mediate cell-to-cell communication and virus transmission [11, 12]. They can change the microenvironment at the site of viral infection, transmit cell growth and transformation signals, and participate in various pathological processes in target cells [13, 14]. It could be argued that exosomes play an essential role in virus infection and pathogenicity. In this study, exosomes were isolated and purified from both cells that were infected with PEDV and mock-infected (negative control) cells. They were then sequenced using transcriptomics to study the role of exosomes in the pathogenicity and virulence of PEDV.

Materials And Methods

2.1. Cells and virus

Vero E6 cells were provided by the Military Veterinary Research Institute (Changchun, China). The classic PEDV CV777 strain was purchased from the Collection of Chinese Bacteria and Virus Species (Beijing, China).

2.2. Isolation, purification, and characterization of exosomes

First, Vero E6 cells were cultured in DMEM (HyClone, USA) containing 10% fetal bovine serum until the cells grew to 90%. The culture medium was then discarded, and cells washed with phosphate-buffered saline (PBS). The experimental group was infected with 1 multiplicity of infection (MOI) of PEDV CV777 standard vaccine strain, and the mock infection group was inoculated with the same volume of DMEM. The samples were then incubated for 1 h at 37°C, supplemented with serum-free DMEM, and allowed to culture for a further 48 h. The supernatant was collected and stored at − 80°C. Secondly, we used exosome isolation kits (Umibio Co., Ltd. Shanghai, China) for exosome isolation. Briefly, the sample was centrifuged for 10 min at 4°C to remove cell debris, and the supernatant was filtered through a 0.22 μm filter. Then, a 30 kDa ultrafiltration tube was used to concentrate the exosomes. In accordance with the manufacturer's instructions, a half volume of exosome precipitation agent was added to the sample and incubated overnight at 4°C. The sample was centrifuged at 4 ℃ and 10,000*g* for 1 h. The sediment at the bottom of the centrifuge tube was resuspended in PBS and transferred to the exosome purification filter (EPF) column and centrifuged at 4000*g* for 10 min at 4 ℃ to collect the liquid at the bottom of the tube. As mentioned earlier, the product was further purified by ultracentrifugation[15]. Finally, the exosomes were characterized by transmission electron microscopy (TEM) and Western blotting.

2.3. RNA extraction and transcriptome sequencing

In accordance with the manufacturer's instructions, total RNA was extracted from exosomes obtained from the different treatment groups using a Simply P Total RNA Extraction Kit (BioFlux, China). The quality of total RNA was determined using the Agilent Small RNA Kit on an Agilent 2100 Bioanalyzer. According to the small RNA protocol, small RNAs were subjected to library construction using the Ion Total RNA-Seq Kit v2 (Life Technologies Corp.). Bioanalysis was done on an Agilent 2100, Eukaryote Total RNA Pico Series II, and RNA-Seq analysis on an Illumina Hi Seq 2500 Sequencing System.

2.4. Quantitative real-time RT-PCR (qPCR) analysis

Total RNA was extracted and purified using the BioFlux RNA Extraction Kit (BioFlux Company, Tokyo, Japan). For exosomal microRNA (miR-103a, let-7d, miR-411, miR-345, miR-328-3P) expression analysis, 0.5 mg of total RNA was first reverse-transcribed with the PrimeScript® 1st Strand cDNA Synthesis Kit (BioFlux Company, Tokyo, Japan) according to the standard protocol. qPCR was performed using SYBR®Premix Ex TaqTM II (TaKaRa, Dalian, China) based on the manufacturer's instructions. The primer sequences are shown in Table 1. For mRNA expression analysis, complementary DNA (cDNA) was synthesized using the PrimeScript® 1st Strand cDNA Synthesis Kit (BioFlux Company, Tokyo, Japan) according to the manufacturer's protocol. Briefly, 2.0 μL of the cDNA template was added to a total volume of 20.0 μL containing 10.0 μL of SYBR®Premix Ex TaqTM II (TaKaRa, Dalian, China), 0.4 μL of Rox 6.0 μL of ddH_2O, and 0.8 μL of the forward and reversed primers. The thermal cycling conditions were as follows: (1) pre-denaturation (30 s at 95 ℃); (2) amplification and quantification (40 cycles of 30 s at 94 ℃, 30 s at 60 ℃). The relative expression was given as the ratio of expression of the target gene to the housekeeping gene using the formula $2^{-\triangle\triangle t}$. Relative expression was normalized and given as a ratio to the expression in the control group.

Table 1
Gene primer sequence list

Gene name	microRNA sequence 5'–3'	RT-primer sequence 5'–3'	Forward primer sequence of qPCR 5'–3'	Reverse primer sequence qPCR 5'–3'
miR-103a	AGCAGCAUUGUACAGGGCUAUGA	GTCGTATCCAGTGCAGGGTCCGAGG TATTCGCACTGGATACGACTCATAG	GCGAGCAGCATTGTACAGGG	AGTGCAGGGTCCGAGGT
let-7d	AGAGGUAGUAGGUUGCAUAGUU	GTCGTATCCAGTGCAGGGTCCGAGG TATTCGCACTGGATACGACAACTAT	GCGCGAGAGGTAGTAGGTTGC	AGTGCAGGGTCCGAGGT
miR-411	AAGGGCTTCCTCTCTGCAGGA	GTCGTATCCAGTGCAGGGTCCGAGG TATTCGCACTGGATACGACTCCTGC	CGCGAAGGGCTTCCTCTCT	AGTGCAGGGTCCGAGGT
miR-345	AGTGCTCCAGGGCTGCGCCTGA	GTCGTATCCAGTGCAGGGTCCGAG GTATTCGCACTGGATACGACTCAGGC	CGAGTGCTCCAGGGCTGC	AGTGCAGGGTCCGAGGT
miR-328-3P	CTGGCCCTCTCTGCCCTTCCG	GTCGTATCCAGTGCAGGGTCCGAGGTA TTCGCACTGGATACGACCGGAAG	CGCTGGCCCTCTCTGCC	AGTGCAGGGTCCGAGGT
ZO-3			CTGTGGTTGTGTCTGACGTGGTAC	GGCTATCTTGACGCAGG
ZO-3-WT			ATCTCTGGAGGCCGAGACCGGCC CGGTGGATCCATGGTTGTATCTGA CGTGGTACCTGGAGGGCC	CCGTTCACCATGACGATC CCTGTCTGTAGCCTGCC GGCCCTCCAGGTACCAC
ZO-3-MUT			ATCTCTGGAGGCCGAGACCGGCCC GGTGGATCCATGGTTGTATCTGACG TGGTACCTCCTGCCCG	CCGTTCACCATGACGATC CCTGTCTGTAGCCTCGG GGGCAGGAGGTACCAC
PC (ocu-miR-328-3p)			CCGGAAGGGCAGAGAGGGCCAGAC CGGTCGGAAGGGCAGAGAGGGCCAGC	TCGAGCTGGCCCTCTCT GACCGGTCTGGCCCTCT TCCGGAGCT
Over-ZO-3			CGCCCCCTCACCCTGGT	TGCTGTGAAAATACTCTC GACCAGGTGG

All the above primers were synthesized by Shanghai Shengong Biotechnology Co., Ltd.

2.5. Western blot analysis

Exosomal protein and PEDV nucleocapsid protein (PEDV-N) were detected by Western blotting. Briefly, the protein concentration of exosomes and PEDV-N was detected using the BCA Protein Detection Kit (Biouniquer Technology CO., LTD, Nanjing, China), and 50 μg of protein lysate from each sample was used for further analyses. After SDS-PAGE electrophoresis, the protein was electro-transferred to a polyvinylidene difluoride (PVDF) membrane. Next, 5% skimmed milk powder was used to block nonspecific antibody binding to the membrane for 1 h. Rabbit anti-CD63/TSG101 monoclonal antibody (Abcam, UK), rabbit anti-ZO3 monoclonal antibody (ImmunoWay, China), mouse anti-PEDV-N monoclonal antibody (Medgene Labs, UK), and β-actin primary antibodies (ImmunoWay, China) were added (overnight at 4 ℃). Samples were washed with TBST 3 times, and HRP-labeled Goat Anti-Rabbit IgG and Goat Anti-Mouse IgG (Proteintech, Chicago, USA) were added. Samples were then incubated at room temperature for 1 h, and NC membranes were washed with TBST 3 times. Finally, the blots were visualized with ECL kits (Beyotime, Shanghai, China). The signal intensity was quantified using grayscale analysis software (Image Tool 3.00).

2.6. Virus titer detection and cytopathic observation

The sample to be detected was serially diluted 10-fold. A solution of each concentration was added to each column at 100 μL per well, which was repeated 8 times for each concentration, followed by the addition of 100 μL of 2% DMEM. The control was established in a virus-free medium and cultured at 37°C in 5% CO2. The virus $TCID_{50}$ was calculated using the Reed–Muench formula. The exosomes of the PEDV CV777-infected Vero cells were extracted, and the PEDV-infected Vero cells with or without exosomes were incubated in a 1.3% methylcellulose medium for 48 h. Then, 4% formaldehyde was added overnight at room temperature and cells were stained with crystal violet staining solution. The cytopathic effect (CPE) results were observed through a Leica DMi8 (Leica, Germany) inverted fluorescence microscope.

2.7. Plasmid construction

The GP-miRGLO vector was used for the construction of ZO-3-WT/ZO-3-MUT/PC. First, we used the primers listed in Table 1 to clone the target gene into the cloning site of the GP-miRGLO vector. After the plasmid was transformed into competent cells, the plasmid was then extracted using the Plasmid Large-Scale Extraction Kit (Sigma-Aldrich, China) and used for subsequent experiments. The primers in Table 1 were used to amplify the complete sequence of the ZO-3 gene from Vero E6 cells for cloning into the pLVX-IRES-ZsGreen1 (Clontech, USA) vector. To ensure the fidelity of the gene sequence, we followed the appropriate operating steps for the production and packaging of lentiviral vectors [16]. When Vero E6 cells grew to 80% confluence, the cells were transfected with the lentiviral vector. After 48 h, the cells and supernatant were harvested for the next experiment.

2.8. Transfection of cells

Lipofectamine 2000 (Invitrogen) was used for transfection when the cells had grown to 80% confluence in a 24-well plate. The miRNA, inhibitor (50 nM), and ZO-3-WT/ZO-3-MUT/PC (2 μg) were co-transfected for 24 h. The dual-luciferase experiment was then performed. miRNA mimics and inhibitors (50 nM) were transfected for 24 h, and 1 MOI of PEDV was added for detection of PEDV infection. The siRNA (100) in Table 1 was transfected into the cells produced by the lentiviral vector for 24 hours and then infected with PEDV of 1 MOI, after which the subsequent experiments proceeded.

2.9. Dual-luciferase reporter gene activity assay

The Dual-Luciferase Reporter Assay System Kit (Promega, USA) was used for detection of luciferase activity in accordance with the manufacturer's protocol. The Vero E6 cells were seeded onto 24-well plates 1 day prior to transfection. The cells were transfected with 1.6 μg of the GP-miRGLO reporter construct containing ZO-3-WT/ZO-3-MUT/PC (the primer sequences are shown in Table 1), together with 10 μL miR-328-3p mimic/mock using Lipofectamine 2000 (Thermo Fisher Scientific, USA). The cells were washed and lysed with the passive lysis buffer from the Dual-Luciferase Reporter Assay System (Promega Corp, USA) 48 h after transfection. Luciferase activity was measured in each cell lysate using a Multifunctional Microplate Reader (Tecan, USA). Relative luciferase activity was first normalized with *Renilla* luciferase activity and then compared with that of the respective control.

Results

3.1. Exosomes isolated from PEDV-infected cells enhance PEDV virulence of

In order to study the role of exosomes in PEDV-infected cells, we first isolated exosomes from the supernatants of infected cells. Under TEM, exosomes were observed to have a typical "cup-shaped" morphology and a crescent-shaped outer membrane (Fig. 1A). We carried out detection of two exosomal marker proteins, CD63 and TSG101, for the PEDV infection group and the mock group. The expression of CD63 was observed to significantly increase after PEDV infection (Fig. 1B). Subsequently, we found that adding PEDV-infected exosomes after PEDV infection promoted virus replication (Fig. 1C). Moreover, the PEDV mRNA expression level gradually increased with the increase in concentration of added exosomes (Fig. 1D). Through crystal violet staining, the addition of exosomes after the cells were infected with PEDV served to reveal cytopathic changes (Fig. 1E), and showed that the addition of exosomes to the culture media of PEDV-infected cells promoted PEDV infection.

3.2. PEDV infection affects the expression of miRNA in exosomes

After the extracted exosomes were subjected to microRNA transcriptome sequencing, we found a total of 861 differentially expressed microRNAs (Fig. 2A). After selecting the p-value range of $0.001 \leq P \text{ value} \leq 0.01$ for statistics, we found 26 differentially expressed microRNAs (Fig. 2B). We then used the enrichment factor, Q-value, and the number of genes annotated to the pathway to measure the degree of pathway enrichment (Fig. 2C). Among them, according to the summary statistical analysis of the results, we found that the tight junction (TJ) is of great research significance. We screened microRNAs targeting the TJ pathway from microRNAs with significant differential expression. We screened eight microRNAs, of which miRNA-328-3p was significantly downregulated (Fig. 2D). We randomly selected five differentially expressed microRNAs and verified their expression by qPCR. The results were consistent with the sequencing results, and miRNA-328-3p could significantly downregulate PEDV mRNA expression levels (Fig. 2E). This indicates that the TJ pathway may play an important role in PEDV infection, and miRNA-328-3p may have an essential regulatory capacity.

3.3. The effect of miRNA-328-3p on PEDV infection

To be able to determine whether miR-328-3p was successfully transfected into Vero cells, we used miR-328-3p-mimic/inhibitor labeled with fluorescein amide (FAM) for transfection. Fluorescence microscopy analysis showed that the FAM-miR-328-3p-mimic/inhibitor was successfully transfected based on observation of a green fluorescent signal in the cytoplasm that was seen not in mock-transfected cells (Fig. 3A). This indicates that miR-328-3p mimics/inhibitors designed and synthesized with FAM fluorophores can be successfully transfected into Vero cells. Compared with the mock group, the addition of the miR-328-3p-inhibitor resulted in a significant increase in the expression level of PEDV-N protein and mRNA. By contrast, the addition of miR-328-3p-mimic substantially reduced the expression level of PEDV-N protein (Fig. 3B, C and D). The addition of a miR-328-3p-inhibitor can increase the virus titer of PEDV substantially. Compared with the mock group, the addition of miR-328-3p-mimic yielded no significant difference in effect based on the PEDV titer (Fig. 3E).

3.4. miR-328-3p can target the ZO-3 protein in the TJ pathway

To further confirm that ZO-3 is a direct downstream target of miR-328-3p, we first performed Western blotting and qPCR analysis on Vero cells transfected with miR-328-3p-mimic/inhibitor/mock to evaluate their effects on ZO-3 expression. The results showed that the miR-328-3p-mimic significantly reduced the mRNA and protein expression levels of ZO-3 compared with the mock group, while the miR-328-3p-inhibitor significantly increased the mRNA and protein expression levels of ZO-3 (Fig. 4A–C). These results indicate that miR-328-3p has a negative regulatory effect on the ZO-3 protein with respect to the TJ pathway. At the same time, we further verified the regulatory relationship between miR-328-3p and ZO-3 through the dual-luciferase reporter gene system. The results show that the miR-328-3p group demonstrated significantly lower luciferase activity in the wild-type ZO-3 and positive control (PC) ZO-3 than the mock group but had no effect on the mutant ZO-3 (Fig. 4D). These results demonstrate that the ZO-3 protein is a target protein directly regulated by miR-328-3p.

3.5. Upregulation of ZO-3 protein promotes PEDV infection

In previous experiments, we demonstrated that exosomal miR-328-3p can inhibit infection of Vero cells by PEDV. To determine whether the regulation of PEDV infection by miR-328-3p requires the mediation of the ZO-3 protein, we both silenced or overexpressed ZO-3 in cells. Then, PEDV nucleocapsid protein (PEDV-N) and mRNA were detected in infected cells. The virus $TCID_{50}$ was also characterized. The results show that the expression level of the ZO-3 protein in the si-ZO-3 group was significantly lower than that in the control group. Simultaneously, the expression of N protein and mRNA of the virus was significantly lower than that of the control group, which indicates that the reduction in ZO-3 protein expression inhibited the expression of virus N protein and RNA (Fig. 5A–C). The virus titer test results showed the same trend (Fig. 5D). On the contrary, overexpression of the ZO-3 protein in virus-infected cells was able to significantly upregulate the expression levels of virus N protein and mRNA in infected cells (Fig. 5E–G). At the same time, the virus titer increased significantly (Fig. 5H). These results constitute strong evidence that the ZO-3 protein facilitates PEDV infection.

Discussion

In previous studies, it was shown that exosomes can carry various intracellular regulatory RNAs, including miRNA, sncRNA, and siRNA [17]. Especially after virus infection, the components of exosomes, which may be proteins or noncoding RNA, also change [18]. Exosomes were initially regarded as waste products of cells before they received extensive attention from the scientific community. Studies in recent years have found that they represent a new means of mediating cell-to-cell communication. The identification of exosomes is usually based on the observation of electron microscopy and Western blotting to detect exosomal marker proteins (such as CD63, CD81, TSG101, annexin 5, ICAM1) [19]. In this study, we first extracted exosomes from PEDV-infected or mock-infected cells. We found that regardless of whether cells were PEDV-infected, they could secrete exosomes, but the expression of the exosomal marker protein CD63 in the PEDV cell group was higher than that in the control group. Following this, we added the extracted exosomes to PEDV-infected cells and found that the addition of exosomes was able to upregulate the expression of the PEDV genome and enhance the CPE of PEDV on cells. This indicates that specific components of exosomes can promote the proliferation of PEDV.

We further performed transcriptome sequencing on the extracted exosomes and found 862 microRNAs that were differentially expressed. We found that the TJ pathway may play an essential role in the PEDV infection process through the KEGG pathway annotation, and miRNA-328-3p is related to the TJ pathway. MicroRNA usually affects the interaction between virus and host in a variety of ways. In past studies, it was shown that miRNA-221-5p can target the PEDV genome after PEDV infection and activate the NFκB pathway to inhibit PEDV replication [20]. Moreover, some microRNA can also interact with related proteins in the interferon pathway, thereby affecting interferon expression to be conducive to virus proliferation [21]. In a study on the relationship between miR-122 and *Hepatitis C virus* (HCV), researchers found that miR-122 can promote HCV expansion [22]. Our research discovered that miRNA-328-3p could downregulate PEDV mRNA and N protein and enhance the PEDV virus titer. This indicates that miRNA-328-3p exerts an inhibitory effect on PEDV.

Claudin is widely present in various epithelial cells. It is mainly responsible for sealing the intercellular space to prevent the random entry and exit of the epithelial layer in order to maintain integrity of the epithelial barrier [8]. In past studies, it was found that occludin is essential for PEDV infection [6]. The expression of occludin is also related to the sensitivity of PEDV to cells [6]. Although PEDV and occludin affect each other, there is no direct interaction between them [6]. In our study, we found that miRNA-328-3p can target ZO-3. The addition of miRNA-328-3p can significantly inhibit the protein expression of ZO-3, and the expression of ZO-3 is also closely related to PEDV infection. When ZO-3 was suppressed, PEDV mRNA and N protein expression levels decreased significantly. On the contrary, when the ZO-3 protein was overexpressed, the mRNA level of PEDV and N protein expression increased considerably, results which are related to the virus titer of PEDV. Interestingly, the overexpression of occludin also increases the sensitivity of cells to PEDV [6]. This shows that ZO-3 has a positive regulatory effect on PEDV infection.

Based on these results, we conclude that PEDV infection downregulates the expression of miRNA-238-3p in exosomes secreted by cells. The downregulation of miRNA-238-3p will upregulate the ZO-3 protein and increase the infectivity of PEDV. The mechanism by which PEDV regulates the expression of miRNA-238-3p and the interaction between ZO-3 protein and PEDV in cells is not fully understood, and the interaction between PEDV and the host appears complicated. Therefore, further work is required to address these issues [23]. In short, our study provides further insights into the infection and pathogenicity of PEDV and contributes to research on the mechanism by which PEDV damages the intestine.

Declarations

Acknowledgment:

The present work was supported by the National Natural Science Foundation of China (32072857, China).

Author Contributions:

Han zhao, Jinxin Yang, Kai Wang, and Guixue Hu conceived and designed the experiments. Han zhao, Jinxin Yang and Wei Lian performed the experiments. Han zhao and Jinxin Yang analyzed the data. Zhanding Cui, Dengliang Li, Jiangting Niu, Shuang Zhang, Yanli Zhao, Yanbing Guo and Qian Zhang contributed reagents/materials/analysis tools. Han zhao and Jinxin Yang wrote the paper. Guixue Hu, Wei Lian and Kai Wang requested financial support. All authors read and approved the manuscript.

Conflicts of Interest:

The authors declare no conflicts of interest.

References

1. Chen Y, Zhang Z, Li J, et al (2018) Porcine epidemic diarrhea virus S1 protein is the critical inducer of apoptosis. Virol J 15:170. https://doi.org/10.1186/s12985-018-1078-4
2. Wu Y, Zhang H, Shi Z, et al (2020) Porcine Epidemic Diarrhea Virus nsp15 Antagonizes Interferon Signaling by RNA Degradation of TBK1 and IRF3. Viruses 12:599. https://doi.org/10.3390/v12060599
3. Kaewborisuth C, Koonpaew S, Srisutthisamphan K, et al (2020) PEDV ORF3 Independently Regulates IκB Kinase β-Mediated NF-κB and IFN-β Promoter Activities. Pathogens 9:376. https://doi.org/10.3390/pathogens9050376
4. Zhang Q, Shi K, Yoo D (2016) Suppression of type I interferon production by porcine epidemic diarrhea virus and degradation of CREB-binding protein by nsp1. Virology 489:252–268. https://doi.org/10.1016/j.virol.2015.12.010
5. Zhang Q, Ke H, Blikslager A, et al (2018) Type III Interferon Restriction by Porcine Epidemic Diarrhea Virus and the Role of Viral Protein nsp1 in IRF1 Signaling. J Virol 92:. https://doi.org/10.1128/JVI.01677-17
6. Luo X, Guo L, Zhang J, et al (2017) Tight Junction Protein Occludin Is a Porcine Epidemic Diarrhea Virus Entry Factor. J Virol 91:. https://doi.org/10.1128/JVI.00202-17
7. Zong QF, Huang YJ, Wu LS, et al (2019) Effects of porcine epidemic diarrhea virus infection on tight junction protein gene expression and morphology of the intestinal mucosa in pigs. Pol J Vet Sci 22:345–353. https://doi.org/10.24425/pjvs.2019.129226
8. (2015) Structural alteration of tight and adherens junctions in villous and crypt epithelium of the small and large intestine of conventional nursing piglets infected with porcine epidemic diarrhea virus. Vet Microbiol 177:373–378. https://doi.org/10.1016/j.vetmic.2015.03.022
9. Zhao S, Gao J, Zhu L, Yang Q (2014) Transmissible gastroenteritis virus and porcine epidemic diarrhoea virus infection induces dramatic changes in the tight junctions and microfilaments of polarized IPEC-J2 cells. Virus Res 192:34–45. https://doi.org/10.1016/j.virusres.2014.08.014
10. Valadi H, Ekström K, Bossios A, et al (2007) Exosome-mediated transfer of mRNAs and microRNAs is a novel mechanism of genetic exchange between cells. Nat Cell Biol 9:654–659. https://doi.org/10.1038/ncb1596
11. Chivero ET, Stapleton JT (2015) Tropism of human pegivirus (formerly known as GB virus C/hepatitis G virus) and host immunomodulation: insights into a highly successful viral infection. J Gen Virol 96:1521. https://doi.org/10.1099/vir.0.000086
12. Wang T, Fang L, Zhao F, et al (2018) Exosomes Mediate Intercellular Transmission of Porcine Reproductive and Respiratory Syndrome Virus. J Virol 92:. https://doi.org/10.1128/JVI.01734-17
13. Bernard MA, Zhao H, Yue SC, et al (2014) Novel HIV-1 MiRNAs Stimulate TNFα Release in Human Macrophages via TLR8 Signaling Pathway. PLOS ONE 9:e106006. https://doi.org/10.1371/journal.pone.0106006
14. Dreux M, Garaigorta U, Boyd B, et al (2012) Short-Range Exosomal Transfer of Viral RNA from Infected Cells to Plasmacytoid Dendritic Cells Triggers Innate Immunity. Cell Host Microbe 12:558–570. https://doi.org/10.1016/j.chom.2012.08.010
15. Zhang K, Xu S, Shi X, et al (2019) Exosomes-mediated transmission of foot-and-mouth disease virus in vivo and in vitro. Vet Microbiol 233:164–173. https://doi.org/10.1016/j.vetmic.2019.04.030
16. Li R, Guo L, Gu W, et al (2016) Production of porcine TNFα by ADAM17-mediated cleavage negatively regulates porcine reproductive and respiratory syndrome virus infection. Immunol Res 64:711–720. https://doi.org/10.1007/s12026-015-8772-8
17. Vojtech L, Woo S, Hughes S, et al (2014) Exosomes in human semen carry a distinctive repertoire of small non-coding RNAs with potential regulatory functions. Nucleic Acids Res 42:7290–7304. https://doi.org/10.1093/nar/gku347
18. Chahar HS, Bao X, Casola A (2015) Exosomes and Their Role in the Life Cycle and Pathogenesis of RNA Viruses. Viruses 7:3204–3225. https://doi.org/10.3390/v7062770
19. Mathivanan S, Ji H, Simpson RJ (2010) Exosomes: extracellular organelles important in intercellular communication. J Proteomics 73:1907–1920. https://doi.org/10.1016/j.jprot.2010.06.006
20. Zheng H, Xu L, Liu Y, et al (2018) MicroRNA-221-5p Inhibits Porcine Epidemic Diarrhea Virus Replication by Targeting Genomic Viral RNA and Activating the NF-κB Pathway. Int J Mol Sci 19:3381. https://doi.org/10.3390/ijms19113381
21. Pedersen IM, Cheng G, Wieland S, et al (2007) Interferon modulation of cellular microRNAs as an antiviral mechanism. Nature 449:919–922. https://doi.org/10.1038/nature06205
22. Henke JI, Goergen D, Zheng J, et al (2008) microRNA-122 stimulates translation of hepatitis C virus RNA. EMBO J 27:3300–3310. https://doi.org/10.1038/emboj.2008.244
23. González-Mariscal L, Tapia R, Chamorro D (2008) Crosstalk of tight junction components with signaling pathways. Biochim Biophys Acta 1778:729–756. https://doi.org/10.1016/j.bbamem.2007.08.018

Figures

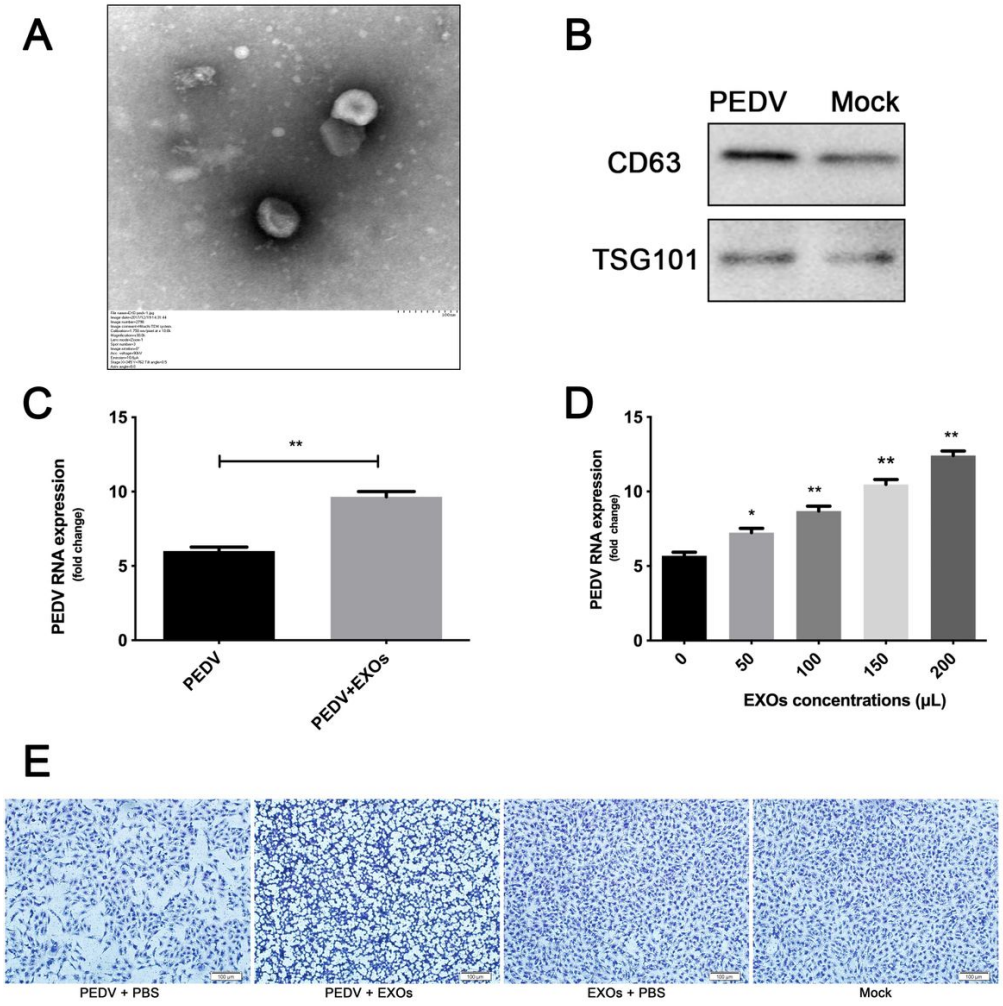

Figure 1

Isolation of exosomes and their effect on PEDV virulence. (A) Image of exosomes observed by TEM after PEDV infection. (B) The expression of the marker proteins CD63 and TSG101 in exosomes of the PEDV infection group and the mock group as detected by Western blotting. (C) The effect of added exosomes on the expression of PEDV RNA as shown by qPCR. (D) The effect of different concentrations of added exosomes on the expression of PEDV RNA as shown by qPCR. (E) The effects of exosomes on CPE after cells were infected with PEDV as shown by crystal violet staining. All experiments were repeated three times. Error bars are expressed as mean with SD; ns < 0.1234; *p < 0.0332; **p < 0.0021.

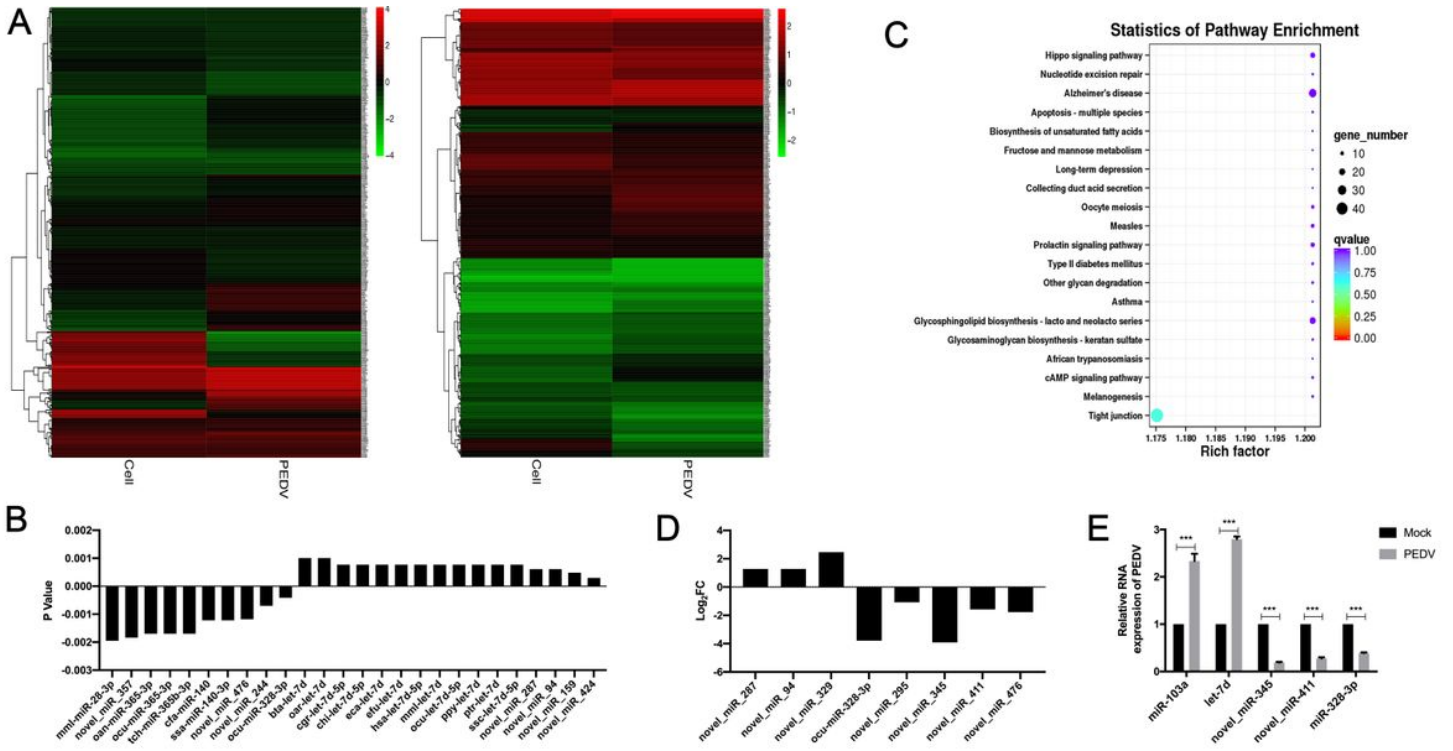

Figure 2

The expression of miRNA-328-3p was detected by transcriptome sequencing, and it was related to the TJ pathway. (A) We used the log10 (TPM+1) value to perform hierarchical cluster analysis of differentially expressed microRNAs with the same or similar expression behavior, and we used online analysis software (www.metaboanalyst.ca) to produce a heat map of differentially expressed microRNA clusters. (B) To further study the relationship between PEDV infection and exosomal microRNA expression, we used $0.001 \leq P \leq 0.01$ as an indicator to screen for microRNAs with significant differences in expression. (C) The degree of pathway enrichment was measured using the enrichment factor, Q-value, and the number of genes annotated to the pathway. We first analyzed the KEGG results using the KOBAS web tool and then used ggplot2 for drawing. We finally obtained a scatter plot of the enrichment of the target gene KEGG pathway. (D) Eight microRNAs with significant differential expression were screened from the microRNAs targeting the TJ pathway. All experiments were repeated three times. (E) We randomly selected five microRNAs for qPCR verification of results. Significant difference analysis showed that ***$p < 0.0002$. The data are derived from three independent experiments, each performed in triplicate. The data are derived from three technical replicates.

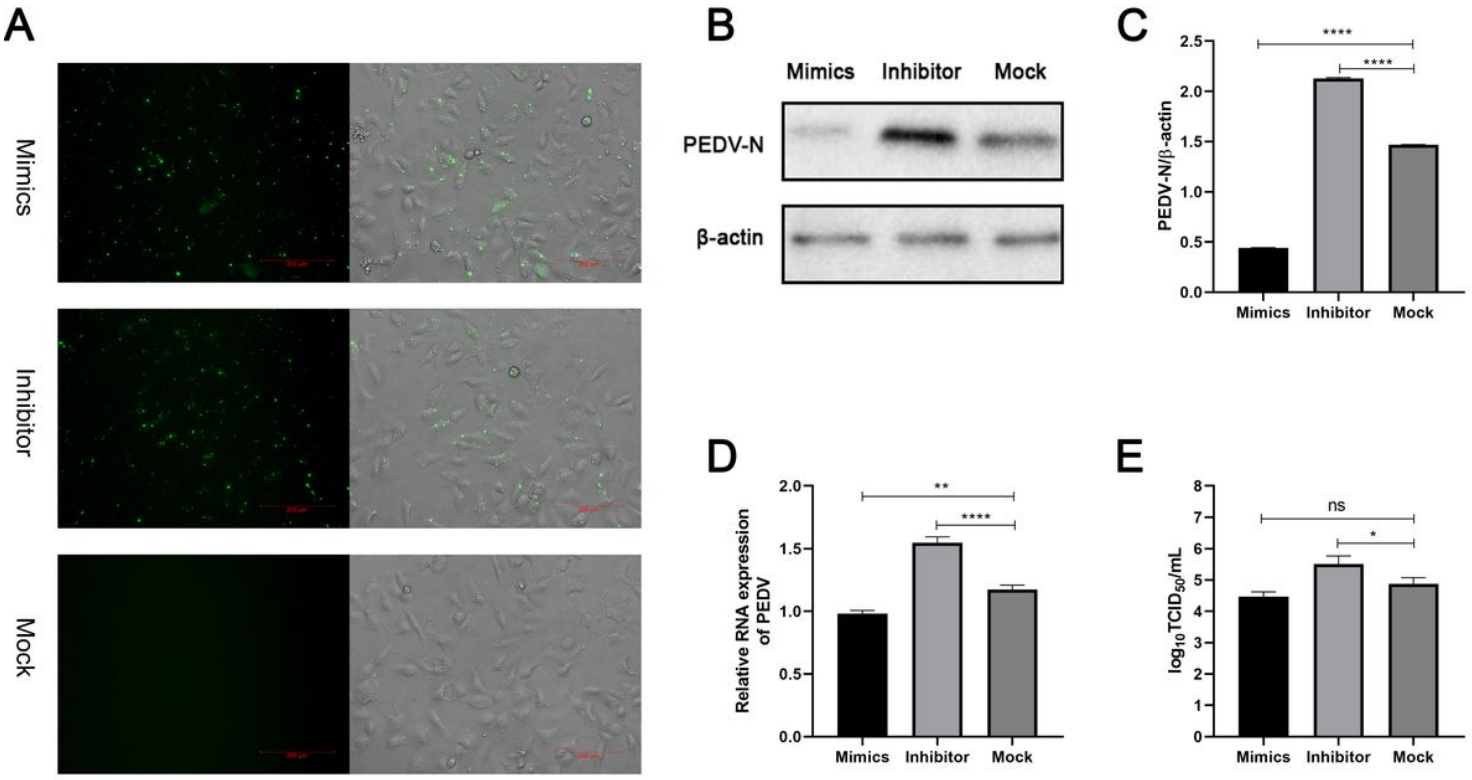

Figure 3

miRNA-328-3p can inhibit PEDV infection. (A) Vero cells were transfected with miR-328-3p mimic/inhibitor with 5`FAM fluorophore. (B) The expression level of PEDV-N protein was detected by Western blotting. (C) We used ImageJ software to normalize PEDV-N protein levels according to β-actin protein levels. (D) The RNA expression level of PEDV was detected by qPCR. (E) The effect of miR-328-3p mimic/inhibitor on PEDV virus titer after transfection. Significant difference analysis showed that ns < 0.1234, *p < 0.0332, **p < 0.0021, ****p < 0.0001. The data are derived from three independent experiments, each performed in triplicate.

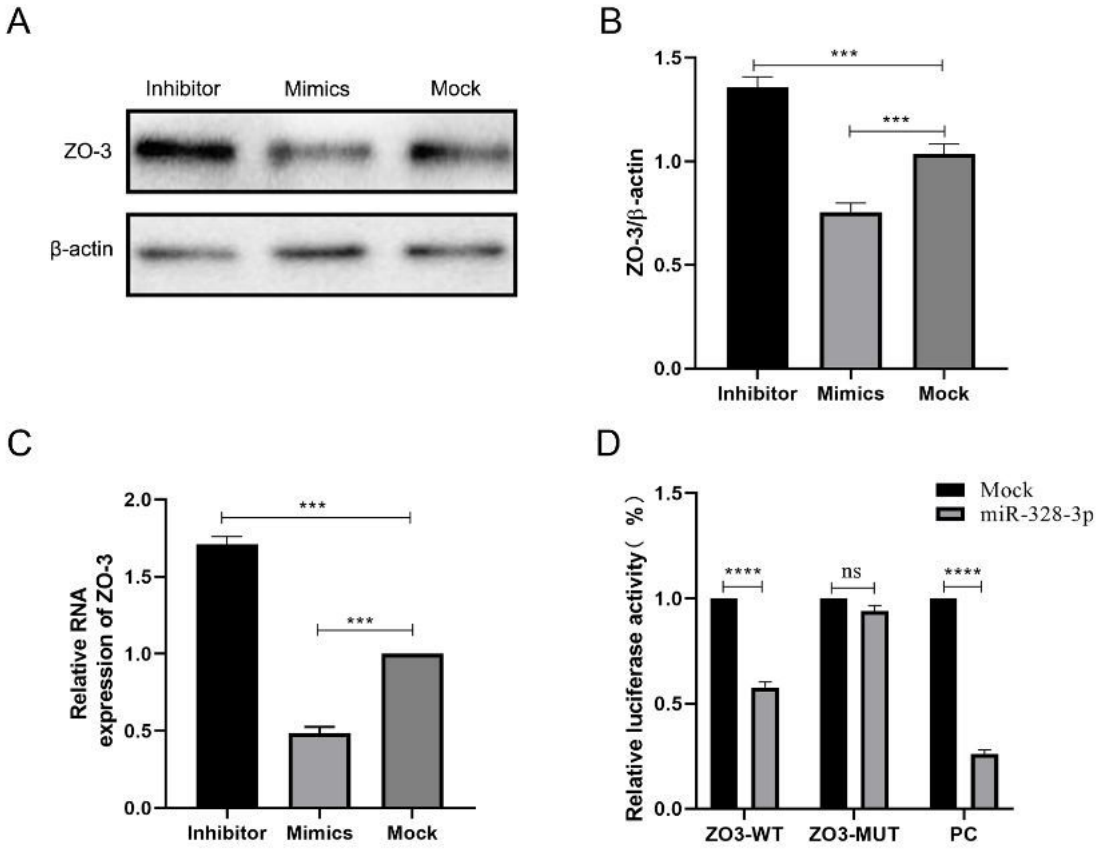

Figure 4

The regulatory effect of exosomal miR-328-3p on ZO-3 protein. (A) The expression of ZO-3 protein was detected by Western blotting. (B) Normalization of ZO-3 protein with endogenous β-actin protein was carried out with ImageJ software. (C) qPCR detection of the genomic RNA expression level of ZO-3. (D) The relationship between miR-328-3p and ZO-3 was detected by dual-luciferase reporter gene activity assay. Significant difference analysis showed that ns < 0.1234, ***p < 0.0002. Data are representative of at least three independent experiments, each performed in triplicate.

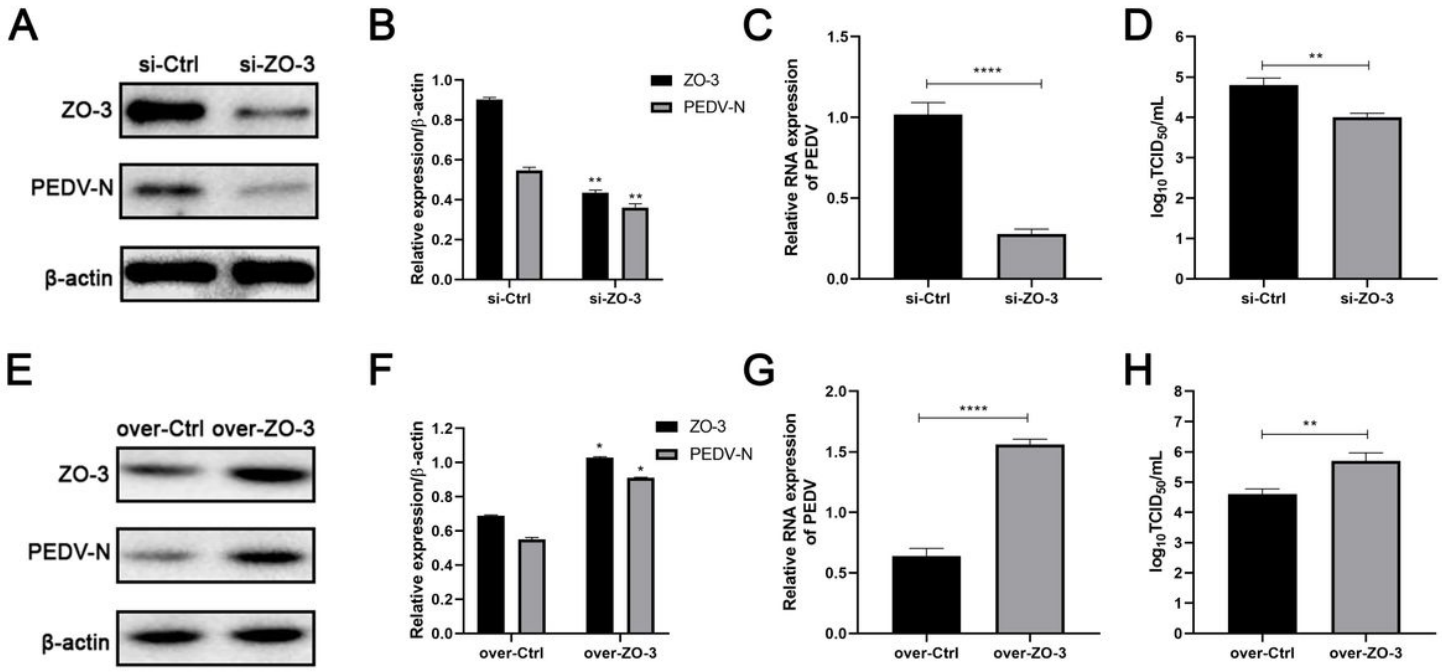

Figure 5

ZO-3 is involved in PEDV infection of cells. (A, E) Si-ZO-3, control interfering RNA (si-Ctrl), over-ZO-3, and control overexpression vector (over-Ctrl) were used to transfect Vero cells. At 48 h post-infection, cell lysates were prepared for detecting ZO-3 and PEDV-N protein expression. (B, F) Normalization of ZO-3 and PEDV-N protein with endogenous protein β-actin was carried out with ImageJ software. (C, G) PEDV genomic RNA levels in si-ZO-3 and over-ZO-3 transfected Vero cells were analyzed by qPCR. (D, H) Virus titers in infected cells were determined at 48 h post-infection. Significant difference analysis showed that *$p < 0.0332$, **$p < 0.0021$, ***$p < 0.0002$. Data are representative of at least three independent experiments, each performed in triplicate.